

Vector analyzing powers for ${}^1\text{H}(\vec{d}, \gamma){}^3\text{He}$ and ${}^2\text{H}(\vec{p}, \gamma){}^3\text{He}$

M. C. Vetterli,* J. A. Kuehner, C. Bamber,[†] N. Davis,[‡] and A. J. Trudel*
Tandem Accelerator Laboratory, McMaster University, Hamilton, Ontario, Canada L8S 4K1

H. R. Weller and R. M. Whitton

Duke University and Triangle Universities Nuclear Laboratory, Durham, North Carolina 27706

(Received 15 March 1988)

The vector analyzing powers for the ${}^1\text{H}(\vec{d}, \gamma){}^3\text{He}$ and ${}^2\text{H}(\vec{p}, \gamma){}^3\text{He}$ reactions have been measured near threshold ($E_\gamma = 7.5$ MeV). The angular distribution of the cross section was also measured for the ${}^2\text{H}(p, \gamma){}^3\text{He}$ reaction. The ratio of the analyzing powers is sensitive to the presence of $S = \frac{3}{2}$ capture strength. It was found that a 10% contribution to the capture by $M1$ radiation (predominantly $S = \frac{3}{2}$) is required to explain the data.

I. INTRODUCTION

Much progress has been made in the last few years on the three-body problem in nuclear physics both theoretically and experimentally. Better wave functions have been obtained by Gibson and Lehman.¹ Sasakawa and Ishikawa have improved the prediction of the binding energy by including three-body forces.² In addition, many data have been obtained for capture reactions leading to three-body systems. In particular for ${}^3\text{He}$, cross sections have been measured for the ${}^2\text{H}(p, \gamma){}^3\text{He}$ reaction by Skopik *et al.*³ and by King *et al.*,^{4,5} and for the ${}^1\text{H}(d, \gamma){}^3\text{He}$ reaction by Belt *et al.*⁶ Furthermore, polarization data have been obtained for proton capture by Skopik *et al.*³ and by King *et al.*⁵ (vector analyzing power A_y), and for deuteron capture by King *et al.*⁵ (A_y) and by Vetterli *et al.*⁷ and Jourdan *et al.*⁸ (tensor analyzing power T_{20}). All of this work shows that a D -state admixture of between 5 and 9% is needed in the ${}^3\text{He}$ ground-state wave function. The polarization data, especially T_{20} , are particularly sensitive to the presence of a D -state component.

This paper reports a measurement of the ratio of the vector analyzing powers for the two reactions ${}^2\text{H}(\vec{p}, \gamma){}^3\text{He}$ and ${}^1\text{H}(\vec{d}, \gamma){}^3\text{He}$ at low energy where the $M1$ contribution is expected to be non-negligible. This work attempts to improve upon a similar comparison by King *et al.*⁵ performed at the somewhat lower energy of $E_x = 6$ MeV. In that work⁵ the deuteron capture data suffered from a large uncertainty due to a high neutron background in the γ detectors which arose from deuteron breakup. In the case of deuteron capture, we avoid this problem by detecting the recoil ${}^3\text{He}$ particles and kinematically inferring the angle of the capture γ ray in a method similar to the one used in Refs. 6 and 7. Both reactions occur predominantly via $E1$ radiation through the $S = \frac{1}{2}$ channel (total spin of the three particles equals $\frac{1}{2}$) to the S -state component of the ${}^3\text{He}$ ground state. The ratio A_d/A_p , where A_d (A_p) is the vector analyzing power for deuteron (proton) capture, has been shown to

be sensitive to the $S = \frac{3}{2}$ capture channel by Seyler and Weller.⁹ Recent calculations which include D -state and meson exchange corrections obtain significant $S = \frac{3}{2}$ $M1$ strength at threshold.¹⁰ The data at $E_x = 6$ MeV (Ref. 5) indicated that $S = \frac{3}{2}$ $M1$ strength was present at the 1–8% level. The present effort was designed to see if this strength persists at higher energy. We derive an experimental value for the ratio A_d/A_p and attempt to interpret it in terms of the presence of $S = \frac{3}{2}$, $M1$ strength at an excitation energy of 7.5 MeV in ${}^3\text{He}$. Section II describes the methods used to measure A_d and A_p . The results are summarized in Sec. III. This is followed by a description of the analysis for both experiments leading to a value for the ratio A_d/A_p . Finally a discussion of the results in terms of $S = \frac{3}{2}$ capture and $M1$ contributions is given in Sec. IV.

II. EXPERIMENTAL METHOD

A. ${}^1\text{H}(\vec{d}, \gamma){}^3\text{He}$

This experiment was done at the Tandem Accelerator Laboratory of McMaster University. Polarized deuterons were produced in a Lamb shift ion source using the spin filter technique¹¹ and accelerated to a laboratory energy of 6 MeV by a model FN tandem Van de Graaff accelerator. This corresponds to a γ -ray energy of 7.5 MeV in the reaction. Several factors determined this choice of energy: (i) the need to be as close as possible to threshold ($E_\gamma \approx 5.5$ MeV) to maximize the $M1$ contribution, (ii) the dramatic reduction in the cross section from its value at $E_\gamma = 12$ MeV, the peak in the capture rate, down to threshold, and (iii) the need to have sufficient energy to allow the ${}^3\text{He}$ particles to escape the target with an acceptable energy resolution. The latter point is important because, as mentioned above, the recoil ${}^3\text{He}$ particles were detected instead of the γ rays to eliminate the large neutron background in NaI detectors from the breakup of the deuterons in the beam. An average beam current of 60 nA was used. This was monitored by means of the

$^{12}\text{C}(\vec{d}, d)^{12}\text{C}_{\text{GS}}$ reaction. Two surface barrier particle detectors were placed symmetrically on either side of the beam in the target chamber. The yields for the ground-state peak for both detectors were summed to eliminate the effect of the analyzing power when the spin of the beam was flipped. This monitoring was possible because the targets were polyethylene films ($\approx 200 \mu\text{g}/\text{cm}^2$) which contain carbon. The average beam polarization was determined to be $(75 \pm 5)\%$ by the quench ratio method. This consists of taking the beam off the spin substate resonance in the spin filter by changing the magnetic field in the cavity. The quench ratio Q is defined as the ratio of the beam current on resonance to the current off resonance. The polarization is then obtained from the relation $p_y = 1 - 1/Q$. For more details see Ref. 12: **B** field quenching. The recoil ^3He particles were momentum analyzed in an Enge split pole magnetic spectrograph positioned at 0° . Since the emitted particles are kinematically constrained to directions less than 3° with respect to the beam, the latter was also let into the spectrograph and focused at the large radius of curvature (ρ) end of the focal plane where it was collected in a Faraday cup. The ^3He particles were focused onto two position sensitive solid-state detectors at the low ρ end. These detectors had dimensions of $45 \text{ mm} \times 8 \text{ mm} \times 100 \mu$ and intrinsic position and energy resolutions of 0.5 mm and 55 keV . However, because of energy loss in the target, the resolution was $\approx 150 \text{ keV}$. Since it was impossible to cover the entire energy range of the ^3He particles with only two detectors in one geometrical arrangement, they were offset and displaced halfway through the experiment as shown in Fig. 1. The position spectra for each detector are shown in Fig. 2. Since we were measuring vector analyzing powers, one side of the spectrometer acceptance was blocked off because the left-right asymmetry in the reaction would have canceled the effect of changing the direction of the spin of the incoming deuterons. The angular acceptance for the spectrometer was $\pm 4.3^\circ$ in θ and $\pm 0.6^\circ$ in ϕ . The small acceptance in ϕ ensures that the polarization of the deuteron beam is perpendicular to $\mathbf{k}_f - \mathbf{k}_i$ where \mathbf{k}_i (\mathbf{k}_f) is the incoming (outgoing) momentum. Therefore the ϕ correction is negligible. The total energy signal from the detectors was used for particle identification. The ^3He peak was well separated as shown in Fig. 3. The energy of the particles was determined from their position on the focal plane. There is a one to one kinematic relationship between the energy of the ^3He particles and the angle of the capture γ ray.^{6,7} This is shown in Fig. 4. An angular distribution of the γ rays can therefore be deduced from the ^3He energy spectrum. This is the same method used in our previous measurement of T_{20} .^{7,13}

B. $^2\text{H}(\vec{p}, \gamma)^3\text{He}$

This reaction was studied at the Triangle Universities Nuclear Physics Laboratory (TUNL) at Duke University. A polarized proton beam was produced by a Lamb shift ion source and accelerated to 3 MeV by a model FN tandem accelerator. This energy was chosen to match the center of mass energy used for the deuteron capture

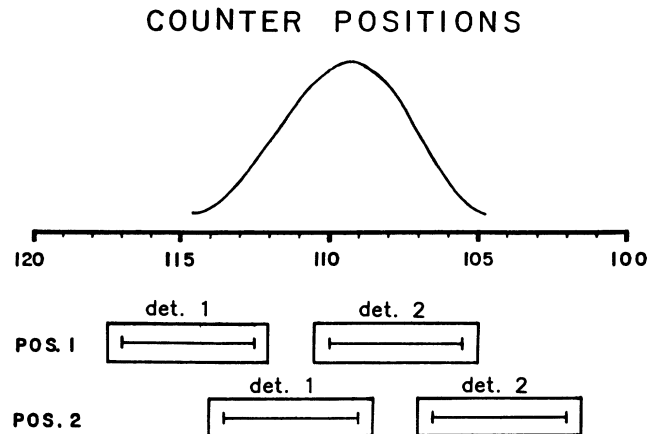


FIG. 1. Setup of the detectors for deuteron capture. Since the active area was not large enough to cover the whole range of ^3He energies, the detectors were moved halfway through the experiment as shown. The scale is in centimeters along the focal plane.

($E_\gamma = 7.5 \text{ MeV}$). The target consisted of a gas cell 16 cm in diameter, containing deuterium at a pressure of 82.7 kPa . The capture γ rays were observed in two large NaI detectors ($25.4 \times 25.4 \text{ cm}^2$) (Ref. 14) which were collimated to view the central region of the gas by means of tungsten and lead absorbers.¹⁵ The length of gas viewed at 90° was 1.9 cm . This arrangement shielded the NaI detectors from background originating from the entrance foil ($0.6 \mu\text{m Ni}$). There was no exit foil; the downstream beam pipe was filled with gas. The beam was pulsed and bunched before injection in order to generate a time-of-flight criterion to help discriminate against neutron events in the NaI detectors. A signal was taken from a capacitive pickup at the exit of the accelerator, and used to stop a time to amplitude converter (TAC) which was

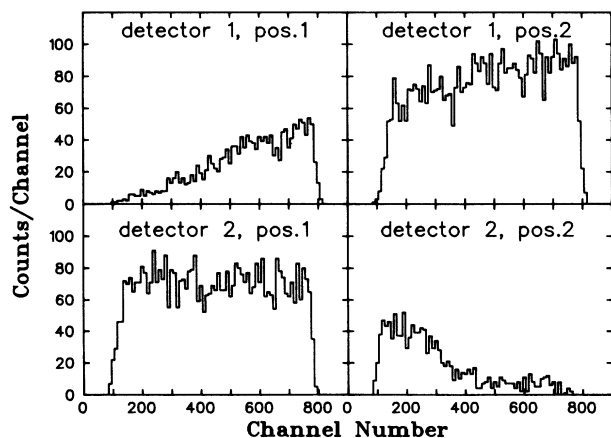


FIG. 2. Raw position spectra from the surface barrier detectors. Refer to Fig. 1 for an explanation of the labeling for the detectors.

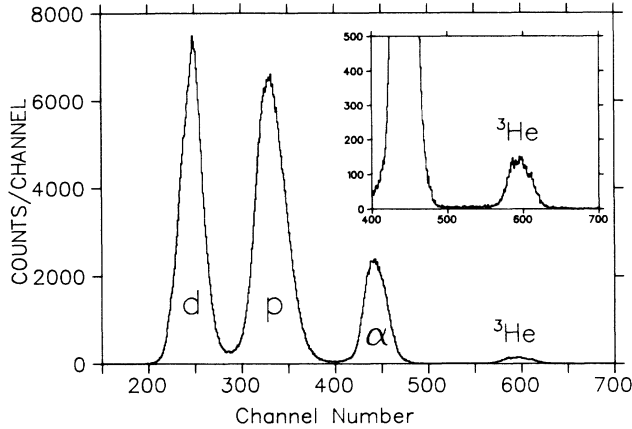


FIG. 3. Spectrum of the total energy loss in the position sensitive solid-state detectors used for the ${}^1\text{H}(\vec{d}, \gamma){}^3\text{He}$ reaction. The ${}^3\text{He}$ peak is well separated as is readily seen in the inset.

started by the NaI signal. The time spectrum showed a peak corresponding to prompt γ rays and a background from events uncorrelated in time (see Fig. 5). The beam was integrated in the beam pipe downstream of the target. This proved unreliable but, in the case of the measurement of $\sigma(\theta)$ with an unpolarized beam, one of the NaI detectors was left at 90° for normalization. The cross-section data were obtained for 12 angles between 30° and 150° . For the analyzing power measurements, the polarization of the beam was determined by the quench ratio method ($p_y = 77\%$). An electric field quenching was used in this case.¹² Analyzing power data were taken for three pairs of angles at 90° , 50° , and 130° with the detectors positioned symmetrically on the left and right sides of the beam. This arrangement eliminates the need for

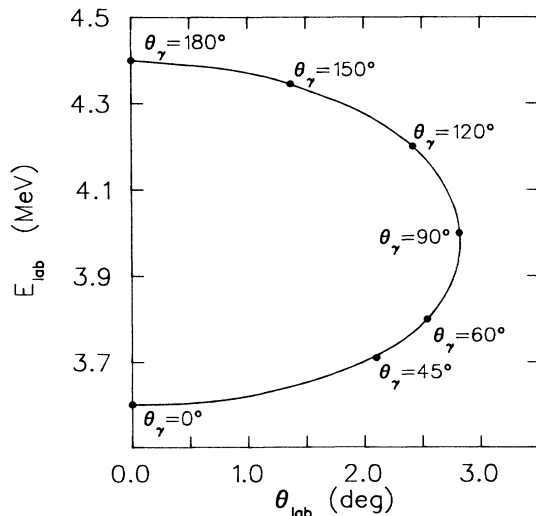


FIG. 4. Kinematic relationship between the energy and the angle of the recoil ${}^3\text{He}$ particles in the lab system. Selected γ -ray angles in the center of mass system are also shown.

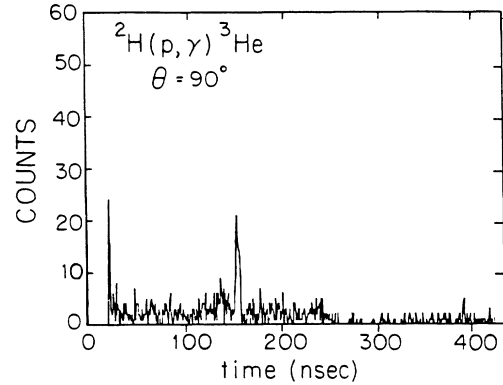


FIG. 5. Timing spectrum for the ${}^2\text{H}(\vec{p}, \gamma){}^3\text{He}$ reaction. The TAC was started by the NaI detector and stopped by a signal from a capacitive pickup at the exit of the accelerator. The prompt γ -ray peak is prominent.

accurate integration of the beam current. A γ -ray energy spectrum for one of the two NaI detectors in the configuration ($90^\circ, 90^\circ$) is shown in Fig. 6. The background in this spectrum, which is due mainly to low-energy neutrons, was obtained by setting a gate off the prompt γ -ray peak in the time spectrum (Fig. 5). The γ peak in the background corrected spectra was integrated to give data on the cross section and analyzing power when using unpolarized and polarized beams, respectively.

III. RESULTS

A. ${}^2\text{H}(\vec{p}, \gamma){}^3\text{He}$

The vector analyzing power for protons is given by

$$A_p = A_y = \frac{1}{p_y} \frac{r-1}{r+1}; \quad r^2 = \frac{L_+ R_-}{L_- R_+}$$

where p_y is the beam polarization, L_+ (R_+) is the yield of the NaI detector on the left (right) side of the beam for spin up, and L_- (R_-) is the corresponding yield for spin

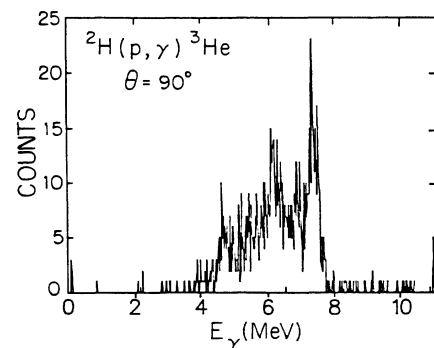


FIG. 6. Energy spectrum for the γ rays observed in the ${}^2\text{H}(\vec{p}, \gamma){}^3\text{He}$ reaction at $E_x = 7.5$ MeV.

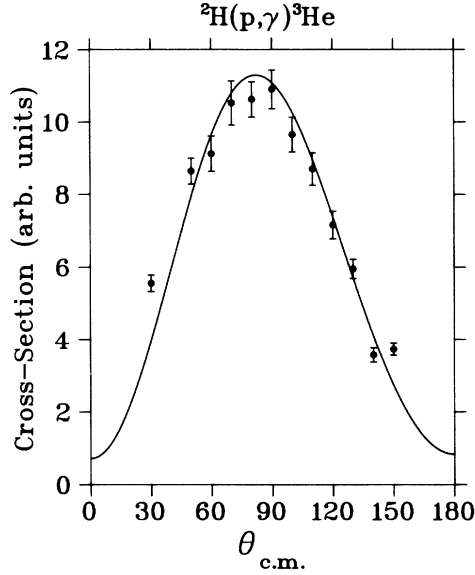


FIG. 7. Angular distribution of the cross section for ${}^2\text{H}(p,\gamma){}^3\text{He}$ in arbitrary units. The curve is the result of a fit to the data expanded in a Legendre polynomial series. See the text for more details.

down. The cross-section angular distribution is plotted in Fig. 7; the analyzing power data are listed in Table I and plotted in Fig. 8.

B. ${}^1\text{H}(\vec{d},\gamma){}^3\text{He}$

The vector analyzing power for a deuteron beam is defined as

$$A_d = A_y = \frac{\sigma_{\text{up}} - \sigma_{\text{down}}}{3\sigma_{\text{un}}p_y}.$$

In this equation σ_{up} (σ_{down}) is the yield for a spin up (down) beam, p_y is the polarization of the beam, and σ_{un} is the unpolarized cross section. The ${}^3\text{He}$ spectra were divided into seven energy bins. Corresponding bins in center of mass γ -ray angle were deduced from kinematics (see Fig. 4). The energy resolution of 150 keV for the ${}^3\text{He}$ particles gives a resolution of approximately 20° for γ -ray

TABLE I. Analyzing power data for ${}^1\text{H}(\vec{d},\gamma)$ and ${}^2\text{H}(\vec{p},\gamma)$ at $E_x = 7.5$ MeV. Note that angles corresponding to deuteron capture are used.

Deuteron capture			Proton capture		
Θ_{cm}	A_d	ΔA_d	Θ_{cm}	A_p	ΔA_p
13°	-0.057	0.01	131°	0.050	0.022
40°	-0.058	0.007	92°	0.039	0.020
60°	-0.048	0.004	92°	0.056	0.027
80°	-0.042	0.004	51°	0.060	0.025
110°	-0.037	0.006			
135°	-0.036	0.006			
162°	-0.014	0.009			

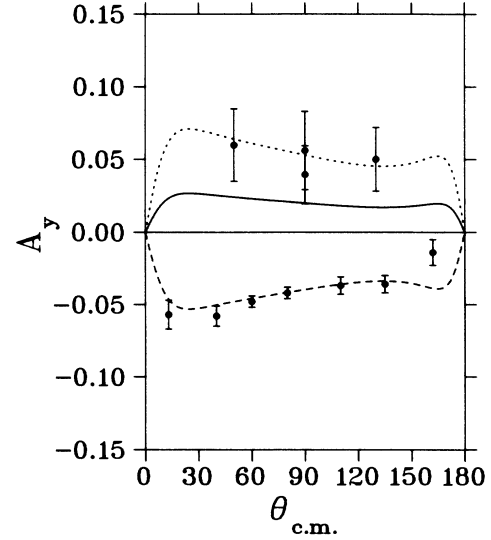


FIG. 8. Analyzing powers for proton capture (positive values) and deuteron capture (negative values) at $E_x = 7.5$ MeV in ${}^3\text{He}$. The dashed curve is the result of a Legendre polynomial expansion of the angular distribution for deuteron capture. The solid curve is -0.5 times the dashed curve and corresponds to the predicted analyzing power for proton capture if only the $S = \frac{1}{2}$ channel is considered. The dotted curve is $-\frac{4}{3}$ times the dashed curve. Note that angles corresponding to deuteron capture are used.

angles near 90° . This binning is implicit in all plots of quantities for the ${}^1\text{H}(\vec{d},\gamma){}^3\text{He}$ reaction. The results for the vector analyzing power are plotted in Fig. 8 and listed in Table I.

IV. DATA ANALYSIS

The observables of the polarized capture experiment can be expanded into Legendre polynomial series.⁹ For an incident polarized proton beam we have

$$\sigma_p(\theta) = \sigma_{pu} [1 + p_y A_p(\theta)],$$

where σ_p is the observed cross section, σ_{pu} is the unpolarized cross section, p_y is the beam polarization, and A_p is the analyzing power for protons. The cross section can also be written as

$$\sigma_{pu}(\theta) = A_0 \left[1 + \sum_{k>1} a_k P_k(\cos\theta) \right].$$

It can also be shown that the following equation holds for the analyzing power:

$$A_p(\theta) \sigma_{pu}(\theta) = A_0 \left[\sum_{k=1} b_k P_k^1(\cos\theta) \right].$$

The corresponding equations for a polarized deuteron beam are

$$\sigma_d(\theta) = \sigma_{du}(\theta) \left[1 + \frac{3}{2} p_y A_d(\theta) \right],$$

$$\sigma_{du}(\theta) = A_0 \left[1 + \sum_{k>1} a_k P_k(\cos\theta) \right],$$

TABLE II. Expansion coefficients for the ${}^2\text{H}(p,\gamma){}^3\text{He}$ cross section.

	This work $E_p = 3.0$ MeV	King <i>et al.</i> ⁵ $E_p = 0.77$ MeV
a_1	0.15 ± 0.02	0.04 ± 0.02
a_2	-0.90 ± 0.03	-0.96 ± 0.02
a_3	-0.16 ± 0.02	-0.07 ± 0.02

and

$$\frac{3}{2} A_d(\theta) \sigma_{du}(\theta) = A_0 \left[\sum_{k=1} b_k P_k^1(\cos\theta) \right].$$

The unpolarized cross section used in the expansion for both reactions was that obtained for proton capture. It is easily shown that the deuteron capture angular distribution is related to the proton capture angular distribution by

$$a_k(d) = (-1)^k a_k(p).$$

Since the data did not extend below 30° or above 150° , the two data points $\sigma(0^\circ) = \sigma(180^\circ) = 0$ were added to give the correct extreme angle behavior known from other experiments.^{3,4} The a_k coefficients were fitted to the proton capture cross section and the results are listed in Table II where they are compared to the results of King *et al.*⁵ The fitted cross section is plotted in Fig. 7. Since a measurement of the cross section was done previously at TUNL (Refs. 3 and 4) this was not the focus of the present experiment. Therefore, the absolute normalization was not carefully controlled and the cross sections are quoted only in arbitrary units. Note that this affects only the value of A_0 ; the a_k coefficients depend on the

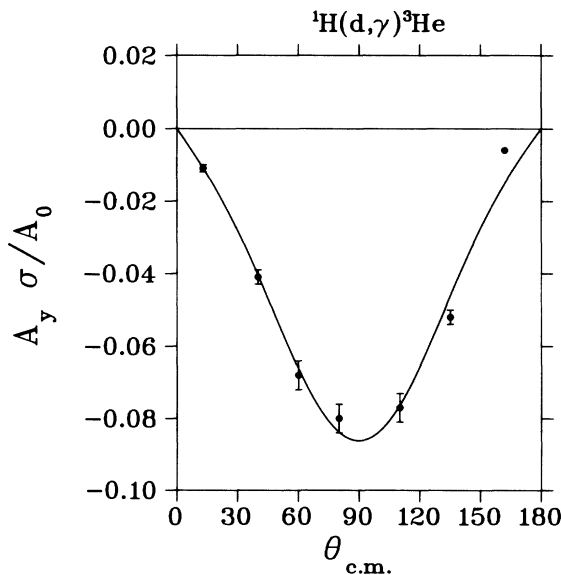


FIG. 9. Angular distribution of the product of analyzing power and cross section for the ${}^1\text{H}(\vec{d},\gamma){}^3\text{He}$ reaction. The curve is the result of a fit to the data expanded in an associated Legendre polynomial series. See the text for more details.

TABLE III. Expansion coefficients for the analyzing power for deuteron capture to ${}^3\text{He}$.

	$E_d = 6.0$ MeV (this work)	$E_d = 1.62$ MeV (King <i>et al.</i> ⁵)
b_1	-0.078 ± 0.003	-0.006 ± 0.045
b_2	0.000 ± 0.002	$+0.018 \pm 0.036$
b_3	0.005 ± 0.002	-0.018 ± 0.036

shape of the angular distribution. If the capture proceeds entirely through $E1$ transitions, we expect the angular distribution to have a $\sin^2(\theta)$ angular dependence. However, the measured distribution is not symmetric about 90° ; this is due to the presence of other multipoles. This was the focus of the work in Ref. 5.

As shown above, $\frac{3}{2} A_y(\theta) \sigma(\theta) / A_0$ for deuteron capture can be expanded in a series of associated Legendre polynomials. This quantity is plotted in Fig. 9 along with the fitted curve. The b_k coefficients are given in Table III along with the results for deuteron capture at $E_d = 1.6$ MeV from Ref. 5. The present data are clearly more precise. From the expressions for the Legendre polynomial expansion of the cross section and the analyzing power, we can write

$$A_d = \frac{2}{3} \frac{\sum b_k P_k^1}{1 + \sum a_k P_k}.$$

This quantity can be calculated using the fitted values for the a_k and b_k , remembering to change the sign of the odd- k a_k coefficients to transform from proton capture to deuteron capture. The result is shown in Fig. 8 where the analyzing powers for deuteron capture (negative values) and proton capture (positive values) are plotted. Note that angles corresponding to deuteron capture are used here. The dashed curve is generated with the fitted parameters for A_d . For pure $S = \frac{1}{2}$ capture, we have^{5,9}

$$\frac{b_k(d)}{b_k(p)} = -3 \Rightarrow \frac{A_d}{A_p} = -2.$$

The solid line of Fig. 8 is obtained by multiplying the dashed line by -0.5 (i.e., pure $S = \frac{1}{2}$ capture). It is obvious that some $S = \frac{3}{2}$ capture is necessary to explain the data. The dotted curve in Fig. 8 is for $-\frac{4}{3} A_d$. The data therefore imply that

$$\frac{\sum b_k(d) P_k^1(\cos\theta)}{\sum b_k(p) P_k^1(\cos\theta)} \approx -2.0.$$

Since $b_k \approx 0$ for $k \neq 1$, we have

$$\frac{b_1(d)}{b_1(p)} \approx -2.0.$$

V. DISCUSSION

An effective two-body direct-capture calculation, similar to that used by King *et al.*,⁴ was done. In the long-wavelength approximation, the radial matrix elements

can be written $R \approx \langle \psi | q_{\text{eff}} r^L | \phi \rangle$, where ψ is the final bound state and ϕ is the initial continuum wave function; q_{eff} is an effective charge. The ψ are two-body $p+d$ wave functions projected from the three-body wave functions of Gibson and Lehman¹ which are generated from Faddeev calculations. The particular wave functions used include 7% D state in the deuteron which corresponds to $\approx 9\%$ D state in ${}^3\text{He}$. The wave functions ϕ are obtained by solving Schrödinger's equation for an optical model potential.¹⁶ The equations relating these matrix elements to the coefficients a_k and b_k are given by Seyler and Weller.⁹ The matrix elements for $E1$ and $E2$ transitions are calculated. However, the $M1$ matrix elements cannot be obtained with this model because of the nonorthogonality of the initial and final states. Therefore, the contribution of $M1$ capture is fitted to the data. In order to simplify the calculations, only $E1$ P waves, $E2$ S and D waves, and $M1$ S waves are used.

The first result is that a pure $E1, E2$ model does not reproduce the b_k coefficients. This is expected because $E2$ capture is greatly reduced at these energies due to the centrifugal barrier. We therefore ignore $E2$ radiation in analyzing the b_k coefficients and use the $M1$ matrix elements as parameters to perform a fit to the data. The cross section is dominated by $E1$ capture while the analyzing power arises from $E1$ - $M1$ interference. Hence the largest $M1$ effects will be found in the b_k coefficients ($b_k=0$ for pure $E1$).

The following procedure was used. The direct-capture model provides the $E1$ amplitudes and phases. Since b_1 is the primary term requiring another amplitude, the equations for $b_1(d)$ and $b_1(p)$ are used to determine the amount of $M1$ strength needed to fit the analyzing

powers. $M1$ strength is introduced into the expressions for $b_1(d)$ and $b_1(p)$ with both $S=\frac{1}{2}$ and $S=\frac{3}{2}$ S -wave capture. The other coefficients were calculated with the deduced $M1$ solution and only a_1 was not reproduced. However, the inclusion of $E2$, as predicted by the model, gives a satisfactory fit to a_1 with essentially no impact on the b_k coefficients. Although the $M1$ solution found is not unique, the results show that the data are consistent with the assumption of a 10% $M1$ contribution which is predominantly ($\approx 95\%$) $S=\frac{3}{2}$.

VI. CONCLUSIONS

The angular distributions of the vector analyzing powers were measured for the ${}^1\text{H}(\vec{d}, \gamma){}^3\text{He}$ and ${}^2\text{H}(\vec{p}, \gamma){}^3\text{He}$ reactions at beam energies corresponding to an excitation energy of 7.5 MeV in ${}^3\text{He}$. A comparison of these indicates the presence of $S=\frac{3}{2}$ capture strength. It was found that these data could be fit if a 10% $M1$ contribution, which is dominated by $S=\frac{3}{2}$ capture, is introduced in addition to the dominant $E1$ and the weak $E2$ radiation predicted by a direct-capture model.

ACKNOWLEDGMENTS

The authors thank Dr. Gibson and Dr. Lehman for the use of their wave functions. One of us (M.V.) would like to thank Dr. O. Häusser for financial support during the latter stages of this project. This work was funded by grants from the Natural Sciences and Engineering Research Council of Canada and by the US Dept. of Energy (Duke-TUNL DOE Contract No. DE-AC05-76ER01067).

*Present address: TRIUMF, 4004 Wesbrook Mall, Vancouver, B.C., Canada V6T 2A3.

†Present address: Department of Physics, University of Rochester, Rochester, NY 14627.

‡Present address: Department of Physics, University of Edinburgh, Mayfield Rd., Edinburgh, Scotland, EH9 3JZ.

¹B. F. Gibson and D. R. Lehman, Phys. Rev. C **29**, 1017 (1984).

²T. Sasakawa and S. Ishikawa, Few Body Syst. **1**, 3 (1986); S. Ishikawa and T. Sasakawa, *ibid.* **1**, 143 (1986).

³D. M. Skopik, H. R. Weller, N. R. Roberson, and S. A. Wender, Phys. Rev. C **19**, 601 (1979).

⁴S. E. King, N. R. Roberson, H. R. Weller, and D. R. Tilley, Phys. Rev. Lett. **51**, 877 (1983).

⁵S. King *et al.*, Phys. Rev. C **30**, 1335 (1984).

⁶B. D. Belt, C. R. Bingham, M. L. Halbert, and A. van der

Woude, Phys. Rev. Lett. **24**, 1120 (1970).

⁷M. C. Vetterli *et al.*, Phys. Rev. Lett. **54**, 1129 (1985).

⁸J. Jourdan *et al.*, Nucl. Phys. **A453**, 220 (1986).

⁹R. G. Seyler and H. R. Weller, Phys. Rev. C **20**, 453 (1979).

¹⁰J. Torre and B. Goulard, Phys. Rev. C **28**, 529 (1983).

¹¹J. L. McKibben, G. P. Lawrence, and G. G. Ohlsen, Phys. Rev. Lett. **20**, 1180 (1968).

¹²G. G. Ohlsen, Los Alamos National Laboratory Report No. LA-4451, 1970.

¹³M. C. Vetterli, Ph.D. thesis, McMaster University, 1985.

¹⁴H. R. Weller and N. R. Roberson, IEEE Trans. Nucl. Sci. **NS-28**, 1268 (1981).

¹⁵S. E. King, N. R. Roberson, H. R. Weller, and D. R. Tilley, Phys. Rev. C **30**, 21 (1984).

¹⁶S. E. King, Ph.D. thesis, Duke University, 1983.